Functional designed to include surface effects in self-consistent density functional theory

Rickard Armiento and Ann E. Mattsson

Original Publication:

Rickard Armiento and Ann E. Mattsson, Functional designed to include surface effects in self-consistent density functional theory, 2005, Physical Review B. Condensed Matter and Materials Physics, (72), 8, 085108.
http://dx.doi.org/10.1103/PhysRevB.72.085108

Functional designed to include surface effects in self-consistent density functional theory

R. Armiento[1,*] and A. E. Mattsson[2,†]
[1]*Department of Physics, Royal Institute of Technology, AlbaNova University Center, SE-106 91 Stockholm, Sweden*
[2]*Computational Materials and Molecular Biology MS 1110, Sandia National Laboratories, Albuquerque, New Mexico 87185-1110, USA*
(Received 25 May 2005; published 4 August 2005)

We design a density-functional-theory (DFT) exchange-correlation functional that enables an accurate treatment of systems with electronic surfaces. Surface-specific approximations for both exchange and correlation energies are developed. A subsystem functional approach is then used: an interpolation index combines the surface functional with a functional for interior regions. When the local density approximation is used in the interior, the result is a straightforward functional for use in self-consistent DFT. The functional is validated for two metals (Al, Pt) and one semiconductor (Si) by calculations of (i) established bulk properties (lattice constants and bulk moduli) and (ii) a property where surface effects exist (the vacancy formation energy). Good and coherent results indicate that this functional may serve well as a universal first choice for solid-state systems and that yet improved functionals can be constructed by this approach.

DOI: 10.1103/PhysRevB.72.085108 PACS number(s): 71.15.Mb, 31.15.Ew

I. INTRODUCTION

Kohn-Sham (KS) density functional theory[1] (DFT) is a method for electronic structure calculations of unparalleled versatility throughout physics, chemistry, and biology. In principle, it accounts for all many-body effects of the Schrödinger equation, limited in practice only by the approximation to the universal exchange-correlation (XC) functional. In this paper we present an improved XC functional, created with a methodology entirely from first principles, that incorporates a sophisticated treatment of electronic surfaces—i.e., strongly inhomogeneous electron densities. This directly addresses a weakness of currently popular functionals.[2–4] The result is a systematic improvement of bulk properties of solid state systems and a qualitative improvement for systems with strong surface effects.

The XC functional suggested in the early works on the theoretical foundation of DFT,[1] the local density approximation (LDA), was derived from the properties of a uniform electron gas, but has shown surprisingly wide applicability for real systems. For solid-state calculations the LDA is still often the method of choice. The next level in functional development, the generalized gradient approximations (GGA's), in many cases significantly improves upon the LDA. The GGA functionals popular for solid-state applications[5,6] are constructed to fulfill constraints that have been derived for the true XC functional. However, the resulting functionals improve results in an inconsistent way (see, e.g., Ref. 4). Even worse, these functionals often are less accurate than the LDA for properties involving strong surfaces effects, such as the generalized surfaces of metal monovacancies. Recent work has explained this as a systematic underestimation of the surface-intrinsic energy contribution that, for simple surface geometries, can be estimated by a posteriori procedure.[2,3] A recently developed meta-GGA functional by Tao, Perdew, Staroverov, and Scuseria[7] (TPSS) is able to fulfill yet more constraints of the exact XC functional by allowing for a more complicated electron density dependence (i.e., through the kinetic energy density of the KS quasiparticle wave functions) than the present work does. However, it appears that TPSS does not fully rectify the surface energy problems found for the GGA's. We repeated the post-correction scheme in Ref. 3 for TPSS, using published TPSS jellium XC surface energies,[7] and from this a remaining surface error is predicted.

The present work follows an alternate route to functional development from the traditional path described above. The LDA's use of the uniform electron gas model system leads to physically consistent approximations (e.g., compatible exchange and correlation that compose the XC functional). Our subsystem functional approach,[8] aims to preserve this propitious property of the LDA through the use of region-specific functionals derived from other model systems. A first effort in this direction was made with the local airy gas[9] (LAG). It extends the LDA by an exchange surface treatment derived from the edge electron gas model system,[10] but keeps the LDA correlation. This first step is completed with the optimized, compatible, correlation introduced here. It is in this sequence of functional development, the LDA, LAG, and then our functional, that the contribution of the present work is most clear.

The XC energy functional $E_{xc}[n]$ operates on the ground-state electron density $n(\mathbf{r})$. It is usually decomposed into the XC energy per particle ϵ_{xc},

$$E_{xc}[n(\mathbf{r})] = \int n(\mathbf{r})\epsilon_{xc}(\mathbf{r};[n])d\mathbf{r}. \quad (1)$$

Exchange and correlation parts are treated separately, with $\epsilon_{xc}=\epsilon_x+\epsilon_c$. We put special emphasis on the conventional, *local*, inverse radius of the exchange hole[10] definition of the exchange energy per particle, $\hat{\epsilon}_x$. This is in contrast to expressions based on transformations of Eq. (1) that arbitrarily delocalize ϵ_x and therefore cannot directly be combined with

each other within the same system.[8] The LDA is local in this sense, while common GGA functionals[5,6] are not. The LDA exchange term is, in Rydberg atomic units,

$$\hat{\epsilon}_x^{\mathrm{LDA}}(n(\mathbf{r})) = -3/(2\pi)[3\pi^2 n(\mathbf{r})]^{1/3}. \quad (2)$$

II. FUNCTIONAL CONSTRUCTION

Kohn and Mattsson[10] put forward the Airy electron gas as a suitable model for electronic surfaces. The Airy gas is a model of electrons in a linear potential, $v_{\mathrm{eff}}(\mathbf{r})=Lz$. L sets an overall length scale and $\hat{\epsilon}_x$ and $n(\mathbf{r})$ can be rescaled by $\hat{\epsilon}_{x,0}^{\mathrm{Airy}}=L^{-1/3}\hat{\epsilon}_x(\mathbf{r};[n])$ and $n_0=L^{-1}n(\mathbf{r})$. Parametrizations are constructed from the exact $\hat{\epsilon}_{x,0}^{\mathrm{Airy}}$ and n_0 expressed[11] in Airy functions Ai,

$$\hat{\epsilon}_{x,0}^{\mathrm{Airy}} = \frac{-1}{\pi n_0}\int_{-\infty}^{\infty} d\zeta' \int_0^{\infty} d\chi \int_0^{\infty} d\chi' \frac{g(\sqrt{\chi}\Delta\zeta, \sqrt{\chi'}\Delta\zeta)}{\Delta\zeta^3} \times \mathrm{Ai}(\zeta+\chi)\mathrm{Ai}(\zeta'+\chi)\mathrm{Ai}(\zeta+\chi')\mathrm{Ai}(\zeta'+\chi'), \quad (3)$$

$$n_0 = [\zeta^2\mathrm{Ai}^2(\zeta) - \zeta\mathrm{Ai}'^2(\zeta) - \mathrm{Ai}(\zeta)\mathrm{Ai}'(\zeta)/2]/(3\pi), \quad (4)$$

$$dn_0/d\zeta = [\zeta\mathrm{Ai}^2(\zeta) - \mathrm{Ai}'^2(\zeta)]/(2\pi), \quad (5)$$

where $\zeta=L^{1/3}z$, $\Delta\zeta=|\zeta-\zeta'|$, and

$$g(\eta,\eta') = \eta\eta' \int_0^{\infty} \frac{J_1(\eta t)J_1(\eta' t)}{t\sqrt{1+t^2}}dt. \quad (6)$$

The LAG functional of Vitos *et al.*[9] uses the ϵ_c of the Perdew-Wang (PW) LDA (Ref. 12) combined with $\hat{\epsilon}_x=\hat{\epsilon}_x^{\mathrm{LDA}}F_x^{\mathrm{LAG}}$ from an Airy gas corresponding to a generic system's density $n(\mathbf{r})$ and scaled gradient $s=|\nabla n(\mathbf{r})|/[2(3\pi^2)^{1/3}n^{4/3}(\mathbf{r})]$. The refinement factor is

$$F_x^{\mathrm{LAG}}(s) = 1 + a_\beta s^{a_\alpha}/(1 + a_\gamma s^{a_\alpha})^{a_\delta}, \quad (7)$$

where $a_\alpha=2.626\,712$, $a_\beta=0.041\,106$, $a_\gamma=0.092\,070$, and $a_\delta=0.657\,946$. F_x depends only on s since $n(\mathbf{r})$ just sets a global scale of the model via L. However, far outside the electronic surface, F_x^{LAG} does not reproduce the right limiting behavior. We have derived an improved parametrization by using (i) the leading behavior of the exchange energy far outside the surface,[10] $\hat{\epsilon}_{x,0}^{\mathrm{Airy}}\to -1/(2\zeta)$, (ii) asymptotic expansions of the Airy functions in Eqs. (4) and (5), and (iii) an interpolation that ensures the expression approaches the LDA appropriately in the slowly varying limit,

$$F_x^{\mathrm{LAA}}(s) = (cs^2+1)/(cs^2/F_x^b + 1),$$

$$F_x^b = -1/[\hat{\epsilon}_x^{\mathrm{LDA}}(\tilde{n}_0(s))2\tilde{\tilde{\zeta}}(s)],$$

$$\tilde{\tilde{\zeta}}(s) = \{[(4/3)^{1/3}2\pi/3]^4\tilde{\zeta}(s)^2 + \tilde{\zeta}(s)^4\}^{1/4},$$

$$\tilde{\zeta}(s) = \left[\frac{3}{2}W\left(\frac{s^{3/2}}{2\sqrt{6}}\right)\right]^{2/3}, \quad \tilde{n}_0(s) = \frac{\tilde{\zeta}(s)^{3/2}}{3\pi^2 s^3}, \quad (8)$$

using a superscript LAA for the local Airy approximation, the Lambert W function,[13] and where $c=0.7168$ is from a least-squares fit to the true Airy gas exchange. Figure 1 shows that the improvement of the LAA over the LAG is small in the intermediate region, but pronounced outside the surface.

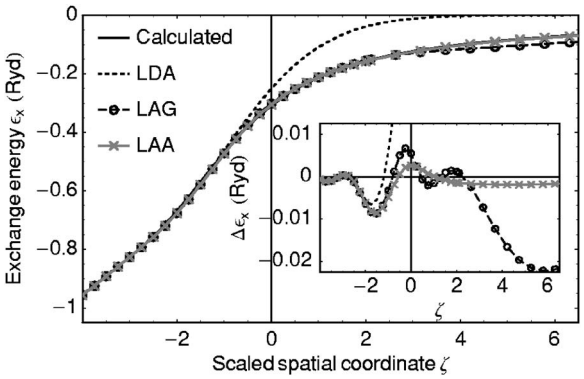

FIG. 1. Parametrizations of Airy exchange $\hat{\epsilon}_x^{\mathrm{Airy}}$ vs scaled spatial coordinate ζ. The solid black line is the true Airy exchange from Eq. (3). The inset shows the difference between the parametrizations and the true exchange. Far outside the edge, the LAA is more accurate than the LAG due to the former's proper limiting behavior.

The Airy exchange parametrizations are designed to accurately model the electron gas at a surface. Hence, they cannot be assumed to successfully work for interior regions. The subsystem functional approach[8] uses an interpolation index for the purpose of categorizing parts of the system as surface or interior regions. We use a simple expression

$$X = 1 - \alpha s^2/(1+\alpha s^2), \quad (9)$$

where α is determined below.

In the present work the LDA is used in the interior. In the limit of low s, the LAG and LAA already approach the LDA exchange. The end result for the interpolated exchange functional is therefore only slightly different from using the LAG or LAA in the whole system. However, interpolation is needed for the correlation and to enable future use of other interior exchange functionals.

No "exact" correlation has been worked out for electrons in a linear potential. To obtain a correlation functional, we combine the LAA or LAG exchange with a correlation based on the LDA, but with a multiplicative factor γ. The numerical value of γ is given by a fit to jellium surface energies σ_{xc}. For a functional $\epsilon_{xc}(\mathbf{r};[n])$, $\sigma_{xc}=\int n(z)[\epsilon_{xc}(\mathbf{r};[n]) - \epsilon_{xc}^{\mathrm{LDA}}(\bar{n})]dz$, where $n(\mathbf{r})$ is from a self-consistent LDA calculation on a system with uniform background of positive charge $\bar{n}$ for $z\leqslant 0$ and 0 for $z>0$ (Ref. 14). The value of $\bar{n}$ is commonly expressed in terms of $r_s=[3/(4\pi\bar{n})]^{1/3}$. The most accurate XC jellium surface energies are given by the improved random-phase approximation scheme presented by Yan *et al.*[15] RPA+. We minimize a least-squares sum $\Sigma_{r_s}|\sigma_{xc}^{\mathrm{approx}}-\sigma_{xc}^{\mathrm{RPA+}}|^2$, using values for $r_s=2.0$, 2.07, 2.3, 2.66, 3.0, 3.28, and 4.0. The surface placement α and the LDA correlation factor γ are fitted simultaneously[16]:

$$\alpha_{\mathrm{LAG}} = 2.843, \quad \gamma_{\mathrm{LAG}} = 0.8228, \quad (10)$$

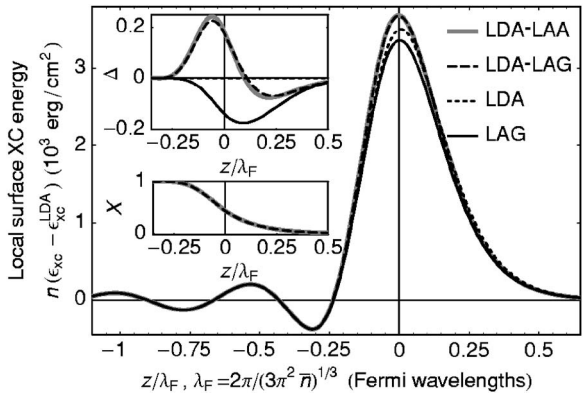

FIG. 2. Local surface XC energy for the $r_s=2.66$ jellium surface. The main figure shows the quantity that integrates to the surface energy σ_{xc} in ergs/cm^2. The upper inset shows the difference between the functionals and LDA. The lower inset shows the interpolation indices X. Integration gives in ergs/cm^2 for LDA 1188, for LAG 1121, and for LDA-LAG(LAA) the "exact" RPA+ value of 1214.

$$\alpha_{\mathrm{LAA}} = 2.804, \quad \gamma_{\mathrm{LAA}} = 0.8098. \tag{11}$$

The resulting fit reproduces the jellium XC surface energies with a mean absolute relative error (MARE) less than half a percent; cf. Fig. 2 and Table I.

The final form of the functional is

$$\hat{\epsilon}_x(\mathbf{r};[n]) = \hat{\epsilon}_x^{\mathrm{LDA}}(n(\mathbf{r}))[X + (1-X)F_x(s)],$$

$$\epsilon_c(\mathbf{r};[n]) = \epsilon_c^{\mathrm{LDA}}(n(\mathbf{r}))[X + (1-X)\gamma], \tag{12}$$

where $F_x(s)$ is either from Eq. (7) or from Eq. (8), and $\epsilon_c^{\mathrm{LDA}}$ is the PW LDA correlation.[12]

III. TESTS

Numerical tests were performed with the plane-wave code SOCORRO.[17,18] Pseudopotentials (PP's) were generated with the FHI98PP code,[19] modified to obtain the XC potential from a numerical functional derivative. We use settings provided by the included element library.[18] The PP's and code modifications have been extensively tested. In addition to the functionals presented by this paper, PP's were generated for the LDA, the GGA of Perdew and Wang (PW91)[5], and the GGA of Perdew, Becke, and Ernzerhof (PBE)[6]. For the latter, bulk calculations with PP's constructed with our numerical functional derivatives agree with the results of PPs based on analytical functional derivatives within 0.001%.[6] We also obtain reasonable agreement with the all-electron bulk results in Ref. 4. As the tools for PP analysis could not easily be made to use numerical derivatives, an analysis was done for PP's of the above functionals with analytical derivatives using identical settings. These PP's were found to have satisfactory logarithmic derivatives and pass the built-in ghost-state tests.[18]

The tests presented here have been chosen from a condensed-matter point of view: three elements for which the LDA and PBE give similar as well as different results. The tests include materials where the GGA (Al) and LDA (Si) are considered to work well. Furthermore, we include a transition metal, Pt, as a more complex material. Established bulk properties are examined to make sure the new functionals do not significantly worsen established results. Then vacancy formation energies are studied, a property known to include strong surface effects and which none of the presently established functionals describe correctly. No other functional has been initially tested on this intricate property.

Bulk properties only include weak surface effects. The equilibrium lattice constant a_0 and bulk modulus $B_0 = -V\partial^2 E/\partial V^2|_{V_0}$ are obtained from the energy minimum given by a fit of seven points in a range about ±10% of the cell volume at equilibrium $V=V_0$ to the Murnaghan equation of state.[20] As seen in Table II our functionals improve on the results of other functionals. A convincing sign of general improvement is the tendency for values to stay between the LDA and PBE, as they are known to overbind and underbind, respectively. As a measure of overall performance, the table shows the mean absolute relative error $\bar{x}$ and its standard deviation $\sigma=[\Sigma(x_i-\bar{x})^2/N]^{1/2}$ for N absolute relative errors x_i. The value of σ gives the spread of the errors independently of their overall magnitude. If further testing confirms the LDA-LAG(LAA)'s robustness to be universal for solid-state systems, they should be considered as a "first

TABLE I. Jellium XC surface energies in erg/cm^2. RPA+ values are from Ref. 15 and are taken as exact. The LDA-LAG and LDA-LAA functionals are created using a two-parameter fit to values for r_s up to 4.00.

r_s	LDA	PW91	PBE	LAG	LDA-LAG	LDA-LAA	RPA+
2.00	3354	3216	3264	3226	3414	3414	3413
2.07	2961	2837	2880	2842	3015	3015	3015
2.30	2019	1929	1960	1926	2058	2058	2060
2.66	1188	1131	1151	1121	1214	1214	1214
3.00	764	725	739	714	782	782	781
3.28	549	521	531	509	563	563	563
4.00	261	247	252	236	269	270	268
5.00	111	104	107	96	115	115	113
MARE	2%	7%	5%	9%	<1%	<1%	

TABLE II. Results of electronic structure calculations for materials exhibiting widely different properties; Al, a free-electron metal; Pt, a transition metal; and Si, a semiconductor. The LDA-LAG and LDA-LAA functionals are from this paper, Eq. (12). Values given as percent are relative errors as compared to experimental values. Values in boldface are mean absolute relative errors. The standard deviation of absolute relative errors σ is defined in the text. LDA-LAG(LAA) are not fitted to any values shown in this table, but to jellium surface energies.

	LDA	PW91	PBE	LAG	LDA-LAG	LDA-LAA	Expt.
Lattice constant of bulk crystal a_0 [Å]							
Pt	3.90	3.99	3.99	3.96	3.93	3.94	3.92[a]
Al	3.96	4.05	4.05	4.02	4.01	4.02	4.03[b]
Si	5.38	5.46	5.47	5.44	5.42	5.43	5.43[c]
Pt	−0.5%	+1.8%	+1.8%	+1.0%	+0.3%	+0.5%	
Al	−1.7%	+0.5%	+0.5%	−0.2%	−0.5%	−0.2%	
Si	−0.9%	+0.6%	+0.7%	+0.2%	−0.2%	0.0%	
	1.0%	**1.0%**	**1.0%**	**0.5%**	**0.3%**	**0.2%**	
σ	0.50	0.59	0.57	0.38	0.12	0.21	
Bulk modulus of bulk crystal B_0 [GPa]							
Pt	312	252	254	272	294	291	283[a]
Al	81.7	72.6	74.9	76.8	82.1	81.7	77.3[b]
Si	95.1	87.5	86.8	88.7	91.5	90.5	98.8[c]
Pt	+10.2%	−11.0%	−10.2%	−3.9%	+3.9%	+2.8%	
Al	+5.7%	−6.1%	−3.1%	−0.6%	+6.2%	+5.7%	
Si	−3.7%	−11.4%	−12.1%	−10.2%	−7.4%	−8.4%	
	6.5%	**9.5%**	**8.5%**	**4.9%**	**5.8%**	**5.6%**	
σ	2.7	2.4	3.9	4.0	1.5	2.3	
Monovacancy formation energy H_V^F [eV]							
Pt	0.91	0.64	0.72	0.73	1.00	0.99	(1.35)[d]
Al	0.67	0.53	0.61	0.59	0.83	0.84	0.68[e]
Si	3.58	3.68	3.65	3.69	3.57	3.59	(3.6)[f]
Atomic XC energies [−hartree]							
Pt	343.92	355.94	354.18	345.76	344.33	344.35	
Al	17.48	18.55	18.43	17.76	17.57	17.59	
Si	19.60	20.78	20.65	19.90	19.69	19.72	

[a]Reference 24.
[b]Reference 2.
[c]Reference 25.
[d]1.35±0.05 eV from Ref. 22.
[e]0.68±0.03 eV from Ref. 2.
[f]3.6±0.2 eV from Ref. 23.

choice" for such applications. Furthermore, an explicit trend is seen in the sequence LDA, LAG, and LDA-LAG(LAA). Throughout the table LAG shifts LDA values towards the PW91/PBE values, while LDA-LAG(LAA) corrects them back towards (and occasionally even beyond) the LDA. This behavior illustrates the importance of compatible correlation.

We now turn to tests of the strong surface effects manifest in calculations of the monovacancy formation enthalpy $H_V^F = E_V - (N-1)E/N$, where E_V and E are total energies for the system with and without a vacancy, and N is the number of atoms in the fully populated supercell. Monovacancy energies are calculated using 64-atom cells. The vacancy cell is geometrically relaxed, and both vacancy and bulk cells are volume relaxed. The number of **k** points used is 4^3 for Pt, 6^3 for Al, and 3^3 for Si. The Si calculations are for the T_d structure.[18] For Pt and Si the supercells are too small for the results to be directly compared to experiment but are sufficient to allow for comparison between functionals.

Strong surface effects are seen for Al and Pt, but not in Si. This is seen by the widely different results between functionals for the metals. Similar to the bulk properties, our surface correlation corrects LAG results in the right direction, but it is apparent that it is still too crude to give truly quantitative results. The surprisingly good LDA result for Al might draw some attention, but as has been pointed out before,[2] it is not reflected in any other property of Al and is thus coincidental.

The unexpected discrepancy between PW91 and PBE monovacancy energies will be addressed in another publication.[21]

We examine only solid-state systems; we do not assess performance for atoms and molecules. However, a hint is provided by the atomic XC energies given from the all-electron calculations used for constructing PP's (cf. Table II). The present functionals give results close to the LDA, with a slight adjustment towards the PBE. For atoms, the PBE is expected to be more accurate than the LDA.[4]

IV. CONCLUSIONS

In conclusion, we have presented two promising functionals for use in DFT calculations. The method of their construction is generic and could potentially be used with *any* local approximation to $\hat{\epsilon}_{xc}$ in the interior region. The locality criteria precludes using, e.g., the PBE for this region,[8] and the effect of a localized equivalent cannot be inferred from GGA results. We are working on a gradient-corrected interior functional and an improved surface correlation. The two varieties of edge treatment, LAG and LAA, behave similarly but we recommend the LAA based on its better behavior far outside the edge.

ACKNOWLEDGMENTS

We are grateful to Thomas R. Mattsson and Peter A. Schultz for valuable help with the electronic structure calculations. R.A. was funded by the project ATOMICS at the Swedish research council SSF. Sandia is a multiprogram laboratory operated by Sandia Corporation, a Lockheed Martin Company, for the U. S. Department of Energy's National Nuclear Security Administration under Contract DE-AC04-94AL85000.

*Electronic address: armiento@mailaps.org
†Electronic address: aematts@sandia.gov

[1] P. Hohenberg and W. Kohn, Phys. Rev. **136**, B864 (1964); W. Kohn and L. J. Sham, Phys. Rev. **140**, A1133 (1965).
[2] K. Carling, G. Wahnström, T. R. Mattsson, A. E. Mattsson, N. Sandberg, and G. Grimvall, Phys. Rev. Lett. **85**, 3862 (2000).
[3] T. R. Mattsson and A. E. Mattsson, Phys. Rev. B **66**, 214110 (2002).
[4] S. Kurth, J. P. Perdew, and P. Blaha, Int. J. Quantum Chem. **75**, 889 (1999).
[5] J. P. Perdew, J. A. Chevary, S. H. Vosko, K. A. Jackson, M. R. Pederson, D. J. Singh, and C. Fiolhais, Phys. Rev. B **46**, 6671 (1992).
[6] J. P. Perdew, K. Burke, and M. Ernzerhof, Phys. Rev. Lett. **77**, 3865 (1996).
[7] J. Tao, J. P. Perdew, V. N. Staroverov, and G. E. Scuseria, Phys. Rev. Lett. **91**, 146401 (2003); V. N. Staroverov, G. E. Scuseria, J. Tao, and J. P. Perdew, Phys. Rev. B **69**, 075102 (2004).
[8] R. Armiento and A. E. Mattsson, Phys. Rev. B **66**, 165117 (2002).
[9] L. Vitos, B. Johansson, J. Kollár, and H. L. Skriver, Phys. Rev. B **62**, 10046 (2000).
[10] W. Kohn and A. E. Mattsson, Phys. Rev. Lett. **81**, 3487 (1998).
[11] Equations (4) and (5) are given by an unconventional method of integration and may be relevant also in other contexts: J. R. Albright, J. Phys. A **10**, 485 (1977); R. Armiento (unpublished).
[12] J. P. Perdew and Y. Wang, Phys. Rev. B **45**, 13244 (1992).
[13] The Lambert *W* function is computed with just a few lines of code; our implementation is available on request: R. M. Corless, G. H. Gonnet, D. E. G. Hare, D. J. Jeffrey, and D. E. Knuth, Adv. Comput. Math. **5**, 329 (1996).
[14] N. D. Lang and W. Kohn, Phys. Rev. B **1**, 4555 (1970).
[15] Z. Yan, J. P. Perdew, and S. Kurth, Phys. Rev. B **61**, 16430 (2000).
[16] Note that this fit is accurate enough to be sensitive to the LDA correlation used (Ref. 12).
[17] SOCORRO is developed at Sandia National Laboratories and available from http://dft.sandia.gov/Socorro/.
[18] See EPAPS Document No. E-PRBMDO-72-020532 for details on the electronic structure calculations. This document can be reached via a direct link in the online article's HTML reference section or via the EPAPS homepage (http://www.aip.org/pubservs/epaps.html).
[19] M. Fuchs and M. Scheffler, Comput. Phys. Commun. **119**, 67 (1999); D. R. Hamann, Phys. Rev. B **40**, 2980 (1989); N. Troullier and J. L. Martins, *ibid.* **43**, 1993 (1991); X. Gonze, R. Stumpf, and M. Scheffler, *ibid.* **44**, 8503 (1991).
[20] F. D. Murnaghan, Proc. Natl. Acad. Sci. U.S.A. **30**, 244 (1944).
[21] A. E. Mattsson, R. Armiento, P. A. Schultz, and T. R. Mattsson (unpublished).
[22] P. Ehrhart, P. Jung, H. Schultz, and H. Ullmaier, *Atomic Defects in Metal*, Vol. 25 of *Landolt-Börnstein*, Group III: *Condensed Matter* (Springer-Verlag, Heidelberg, 1991).
[23] G. D. Watkins and J. W. Corbett, Phys. Rev. **134**, A1359 (1964); E. L. Elkin and G. D. Watkins, Phys. Rev. **174**, 881 (1968).
[24] A. Khein, D. J. Singh, and C. J. Umrigar, Phys. Rev. B **51**, 4105 (1995).
[25] O. Madelung, *Semiconductors*, Vol. 17a of *Landolt-Börnstein*, Group III: *Condensed Matter* (Springer-Verlag, Berlin, 1982).